We are IntechOpen,
the world's leading publisher of
Open Access books
Built by scientists, for scientists

4,800
Open access books available

122,000
International authors and editors

135M
Downloads

154
Countries delivered to

Our authors are among the

TOP 1%
most cited scientists

12.2%
Contributors from top 500 universities

BOOK CITATION INDEX
CLARIVATE ANALYTICS
INDEXED

WEB OF SCIENCE™

Selection of our books indexed in the Book Citation Index
in Web of Science™ Core Collection (BKCI)

Interested in publishing with us?
Contact book.department@intechopen.com

Numbers displayed above are based on latest data collected.
For more information visit www.intechopen.com

Stochastic State Estimation for Simultaneous Localization and Map Building in Mobile Robotics

Juan Andrade Cetto, Teresa A. Vidal Calleja & Alberto Sanfeliu

1. The Problem of Coupled Stochastic

1.1 State Estimation

[1]The study of stochastic models for Simultaneous Localization and Map Building (SLAM) in mobile robotics has been an active research topic for over fifteen years. Within the Kalman filter (KF) approach to SLAM, seminal work (Smith and Cheeseman, 1986) suggested that as successive landmark observations take place, the correlation between the estimates of the location of such landmarks in a map grows continuously. This observation was later ratified (Dissanayake et al., 2001) with a proof showing that the estimated map converges monotonically to a relative map with zero uncertainty. They also showed how the absolute accuracy of the map reaches a lower bound defined only by the initial vehicle uncertainty, and proved it for a one-landmark vehicle with no process noise.

From an estimation theoretic point of view, we address these results as a consequence of partial observability. We show that error free reconstruction of the map state vector is not possible with typical measurement models, regardless of the vehicle model chosen, and show experimentally that the expected error in state estimation is proportional to the number of landmarks used. Error free reconstruction is only possible once full observability is guaranteed.

Explicit solutions to the continuous time SLAM problem for a one-dimensional vehicle called the *monobot* appear in (Gibbens et al., 2000, Kim, 2004). Both give closed form asymptotic values of the state error covariance $\mathbf{P}$. Kim observed that, for the case when not all landmarks are observed at all times, the asymptotic value on the determinant of $\mathbf{P}$ reaches a constant value greater than zero. Gibbens *et al.* on the other hand, observed that the rate of convergence of $\mathbf{P}$ is proportional to the number of landmarks used, and that its asymptotic value is independent of the plant variance. In their solution to the 1-d Brownian motion case, the state error covariance is linked to the total number of landmarks in the form of the total Fisher information $I_T = \sum_1^n \left(1/\sigma_w^2\right)$. The expression indicates the "*informational equivalence of the measurements and the innovations*" (Bar-Shalom et al., 2001), and was derived from a simple likelihood function, one that does not contain the fully correlated characteristics of the measurement model. This Chapter contains a

---

more general expression for the total Fisher information in SLAM that shows explicitly the unobservable directions of the state space.

To speed up the performance of Kalman filterbased SLAM algorithm, some authors have proposed the use of covariance inflation methods for the decorrelation of the state error covariance (Guivant and Nieto, 2003), subject to suboptimality of the filter. Adding pseudo-noise covariance to the landmark states is equivalent to making the system controllable. However, full decorrelation of a partially observable system might lead to filter unstability (Julier, 2003). In this Chapter we also show how to diagonalize only part of the state error covariance to obtain a suboptimal filter that is both linear in time, and stable, at the same time.

In summary; in SLAM, the state space constructed by appending the robot pose and the landmark locations is fully correlated, a situation that hinders full observability. Moreover, the modelling of map states as static landmarks yields a partially controllable state vector. The identification of these problems, and the steps taken to palliate them, are covered in this Chapter.

The Chapter is structured as follows. In Section 2 we present the Simultaneous Localization and Map Building problem as a stochastic state estimation problem, and choose the Extended Kalman Filter algorithm as an alternative for solving it. The steady state of the filter will always depend on the initial noise parameters. The effect of partial observability is known as marginal stability (Todling, 1999), and is in general an undesirable feature in state estimation. In Section 3 we show that marginal filter stability is a consequence of having a coupled state estimation problem, by anylizing the poles of the state error dynamics. In Section 4 we derive an expression for the total Fisher information in SLAM. The analysis yields a closed form solution that shows, explicitly, the unobservable directions of the map state.

Marginal filter stability and the singularity of the Fisher information matrix are equivalently consequences of having partial observability. In Section 5 we develop expressions for the observable and controllable subspaces for a non-holonomic velocity controlled planar mobile platform. The result is that as the number of landmarks increases, the state components get closer to being reconstructible.

In Section 6 we show how partial observability in SLAM can be avoided by adding a fixed external sensor to the state model, or equivalently, by setting a fixed landmark in the environment to serve as global localization reference. Full observability yields the existence of a (not necessarily unique) steady state positive semi-definite solution for the error covariance matrix, guaranteeing a steady flow of the information about each state component, and preventing the uncertainty (error state covariance) from becoming unbounded (Bar-Shalom et al., 2001).

In Section 7 we show how as a consequence of having a partial controllability, filtering of the landmark state estimates is terminated after a small number of iterations, i.e., their corresponding Kalman gain terms tend to zero. In subsection 7.1 we show a situation in which the filter becomes unstable during covariance inflation. In subsection 7.2 we introduce a method for covariance decorrelation that preserves the stability of the filter. Furthermore, we show in subsection 7.3 another solution for a stable covariance inflation algorithm, consisting on first recovering full observability prior to decorrelating the entire state error covariance matrix. Conclusions are presented in Section 8.

2. Kalman Filter Based SLAM
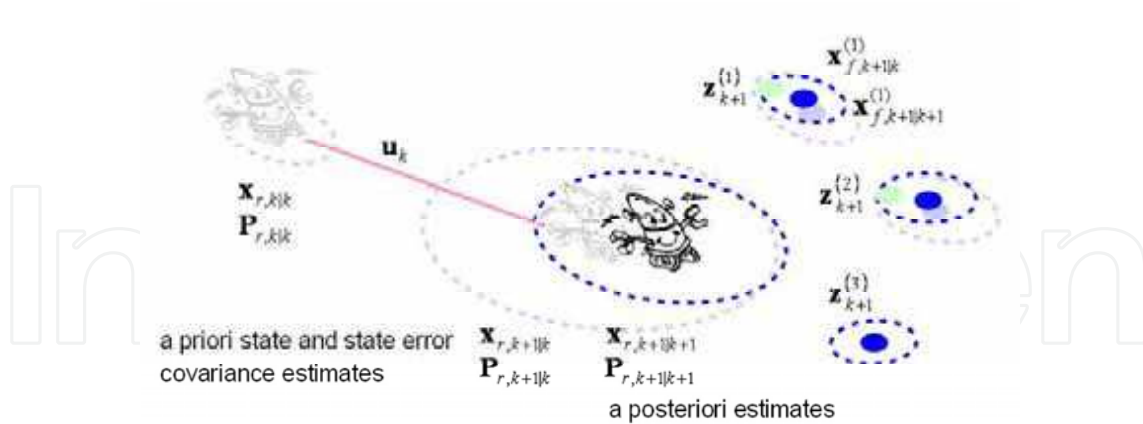
2.1 System Model

Figure 1. State estimation approach to simultaneous localization and map building

Formally speaking, the motion of the robot and the measurement of the map features are governed by the discrete-time state transition model

$$x_{k+1} = f(x_k, u_k, v_k)$$
$$z_k = h(x_k) + w_k \tag{1}$$

The state vector x_k contains the pose of the robot $x_{r,k}$ at time step k, and a vector of stationary map features x_f, i.e.,

$$x_k = \begin{bmatrix} x_{r,k} \\ x_f \end{bmatrix} \tag{3}$$

The input vector $\mathbf{u}_k$ is the vehicle control command, and $\mathbf{v}_k$ and $\mathbf{w}_k$ are Gaussian random vectors with zero mean and psd covariance matrices $\mathbf{Q}$ and $\mathbf{R}$, respectively, representing unmodeled robot dynamics and system noise the former; and measurement noise the latter. See Figure 1.

2.2 Algorithm

Provided the set of observations $Z^k = \{z_1, ..., z_k\}$ was available for the computation of the current map estimate $\mathbf{x}_{k|k}$, the expression

$$x_{k+1|k} = f(x_{k|k}, u_k, 0) \tag{4}$$

gives an a priori noise-free estimate of the new locations of the robot and map features after the vehicle control command $\mathbf{u}_k$ is input to the system. Similarly,

$$\mathbf{z}_{k+1|k} = \mathbf{h}(\mathbf{x}_{k+1|k}) \tag{5}$$

constitutes a noise-free a priori estimate of sensor measurements.

Given that the landmarks are considered stationary, their a priori estimate is simply $x_{f,k+1|k} = x_{f,k|k}$; and the a priori estimate of the map state error covariance showing the increase in robot localization uncertainty is

$$P_{k+1|k} = E\left[\tilde{x}_{k+1|k} \tilde{x}_{k+1|k}^{\mathrm{T}} \right] \tag{6}$$

$$= FP_{k|k}F^T + GQG^T \tag{7}$$

The Jacobian matrices $\mathbf{F}$ and $\mathbf{G}$ contain the partial derivatives of $\mathbf{f}$ with respect to the state $\mathbf{x}$ and the noise $\mathbf{v}$, evaluated at $\left(x_{k|k}, u_k, 0\right)$.

Assuming that a new set of landmark observations $\mathbf{z}_{k+1}$ coming from sensor data has been correctly matched to their map counterparts, one can compute the error between the measurements and the estimates with $\tilde{\mathbf{z}}_{k+1|k} = \mathbf{z}_{k+1} - \mathbf{z}_{k+1|k}$. This error, known as the innovation, aids in revising both the map and robot locations. The a posteriori state estimate is

$$\mathbf{x}_{k+1|k+1} = \mathbf{x}_{k+1|k} + \mathbf{K}\tilde{\mathbf{z}}_{k+1|k} \tag{8}$$

and the Kalman gain is computed with

$$\mathbf{K} = \mathbf{P}_{k+1|k}\mathbf{H}^T\mathbf{S}^{-1} \tag{9}$$

where $\mathbf{S}$ is the measurement innovation matrix,

$$\mathbf{S} = \mathbf{H}\mathbf{P}_{k+1|k}\mathbf{H}^T + \mathbf{R} \tag{10}$$

and $\mathbf{H}$ contains the partial derivatives of the measurement model $\mathbf{h}$ with respect to the state $\mathbf{x}$ evaluated at $(\mathbf{x}_{k+1|k})$.

Finally, the a posteriori estimate of the map state error covariance must also be revised once a measurement has taken place. It is revised with the Joseph form to guarantee positive semi-definiteness.

$$\mathbf{P}_{k+1|k+1} = \left(\mathbf{I} - \mathbf{K}\mathbf{H}\right)\mathbf{P}_{k+1|k}\left(\mathbf{I} - \mathbf{K}\mathbf{H}\right)^T + \mathbf{K}\mathbf{R}\mathbf{K}^T \tag{11}$$

3. Convergence

Substituting the linearized version of (4) in (8), we may rewrite the KF in the one-step ahead prediction form

$$\mathbf{x}_{k+1|k} = \left(\mathbf{F} - \mathbf{K}\mathbf{H}\right)\mathbf{x}_{k|k-1} + \mathbf{K}\mathbf{z}_k \tag{12}$$

and with the appropriate substitutions, using (6) and (12), the corresponding prediction error dynamics becomes

$$\tilde{\mathbf{x}}_{k+1|k} = (\mathbf{F} - \mathbf{K}\mathbf{H})\tilde{\mathbf{x}}_{k|k-1} + \mathbf{G}\mathbf{v}_k - \mathbf{K}\mathbf{w}_k \tag{13}$$

In general, only for a stable matrix $\mathbf{F}\text{-}\mathbf{K}\mathbf{H}$, the estimation error will converge to a zero mean steady state value. However, in SLAM, $\mathbf{F}\text{-}\mathbf{K}\mathbf{H}$ is marginally stable, thus the steady state error estimate is bounded to a constant value, subject to the filter initial conditions. To show $\mathbf{F}\text{-}\mathbf{K}\mathbf{H}$ marginally stable, consider the one landmark monobot from Figure 2. $\mathbf{F}=\mathbf{I}$, $\mathbf{G} = [1,0]^T$, and $\mathbf{H} = [-1,1]$. For any value of

$$\mathbf{P} = \begin{bmatrix} \sigma_r^2 & \rho\sigma_r\sigma_f \\ \rho\sigma_r\sigma_f & \sigma_f^2 \end{bmatrix} \tag{14}$$

the Kalman gain, computed with (9), is

$$K = \frac{1}{s}\begin{bmatrix} -\sigma_v^2 \\ \sigma_w^2 \end{bmatrix} \tag{15}$$

where

$$s = \sigma_r^2 + \sigma_f^2 - 2\rho\sigma_r\sigma_f + \sigma_w^2 \tag{16}$$

is the innovation variance. Consequently,

$$F - KH = \frac{1}{s}\begin{bmatrix} -\sigma_v^2 + s & \sigma_v^2 \\ \sigma_w^2 & -\sigma_w^2 + s \end{bmatrix} \tag{17}$$

with eigenvalues

$$\left\{ \begin{array}{c} 1 \\ \frac{1}{s}\left(s - \sigma_v^2 - \sigma_w^2\right) \end{array} \right\} \quad and \quad s \neq 0$$

One of the eigenvalues being on the unitary circle yields marginal stability, i.e., constant bounded non-zero mean error state estimate convergence. Moreover, the marginal stability of **F-KH** guarantees at least one *psd* steady state solution to the Riccati equation for the one-step ahead state error covariance (Vidal-Calleja et al., 2004b, Kailath et al., 2000).

$$\mathbf{P}_{k+1|k} = (\mathbf{F} - \mathbf{KH})\mathbf{P}_{k|k-1}(\mathbf{F} - \mathbf{KH})^{\mathrm{T}} + \mathbf{GQG}^{\mathrm{T}} + \mathbf{KHRH}^{\mathrm{T}}\mathbf{K}^{\mathrm{T}} \tag{18}$$
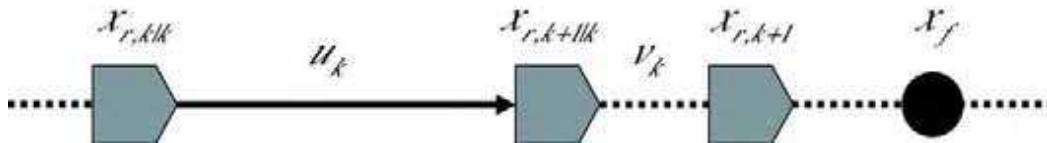

Figure 2. Monobot, a one-dimensional mobile robot

4. Total Fisher Information

Under the Gaussian assumption for the vehicle and sensor noises, and for linear vehicle and measurement models, the Kalman filter is the optimal minimum mean square error estimator. And, as pointed out in (Bar-Shalom et al., 2001), minimizing the least squares criteria $E[\tilde{\mathbf{x}}_{k+1|k+1}\tilde{\mathbf{x}}_{k+1|k+1}^{\mathrm{T}}]$ is equivalent to the maximization of a likelihood function $\wedge(x)$ given the set of observations Z^k; that is, the maximization of the joint probability density function of the entire history of observations

$$\wedge(x) = \prod_{i=1}^{k} p(z_i | Z^{i-1}) \tag{19}$$

where $\mathbf{x}$ is the augmented map state (vehicle and landmark estimates), and $\mathbf{z}_i$ the entire observation vector at time i.

Given that the above pdfs are Gaussian, and that $E[\mathbf{z}_i] = \mathbf{Hx}_{i|i-1}$, the pdf for each measurement in SLAM is

$$p(z_i | Z^{i-1}) = N(\tilde{z}_{i|i-1}; 0, \mathbf{S}_i) \tag{20}$$

with $\mathbf{S}_i = E[\tilde{\mathbf{z}}_{i|i-1}\tilde{\mathbf{z}}_{i|i-1}^{\mathrm{T}}]$.

In practice however, it is more convenient to consider the log likelihood function $\ln \wedge(x)$. The maximum of $\ln \wedge(x)$ is at the value of the state $\mathbf{x}$ that most likely gave rise to the observed data Z^k, and is obtained by setting its derivative with respect to $\mathbf{x}$ equal to zero, which gives

$$\nabla_x \ln \wedge(x) = \sum_{i=1}^{k} H^{\mathrm{T}} S_i^{-1} \tilde{z}_{i|i-1} \tag{21}$$

An intuitive interpretation of the maximum of the log-likelihood is that the best estimate for the state **x**, in the least squares sense, is the one that makes the sum of the entire set of Mahalanobis distances $\sum_{i=1}^{k} \tilde{z}_{i|i-1}^{\mathrm{T}} S_i^{-1} \tilde{z}_{i|i-1}$ as small as possible. A measure that is consistent with the spatial compatibility test described in (Neira and Tardós, 2001). The Fisher information matrix, a quantification of the maximum existing information in the observations about the state **x**, is defined in (Bar-Shalom et al., 2001) as the expectation on the dyad of the gradient of $\ln \wedge(x)$, that is

$$J = E\left[(\nabla_x \ln \Lambda(x))(\nabla_x \ln \Lambda(x))^{\mathrm{T}} \right] \tag{22}$$

Taking the expectation on the innovation error in the above formula gives the sum

$$J = \sum_{i=1}^{k} H^{\mathrm{T}} (HPH^{\mathrm{T}} + R)^{-1} H \tag{23}$$

It is easy to verify that in the linear case, this expression for the total Fisher information is only a function of $P_{r,0|0}$, **Q**, and **R**. If, on the other hand, the EKF is used, the Jacobian **H** in (23) should be evaluated at the true value of the states $x_0, \dots x_k$. Since these are not available, an approximation is obtained at the estimates $\mathbf{x}_{i|i-1}$. The pre and post multiplying **H** is, in this context, also known as the *sensitivity matrix*.

A necessary condition for the estimator (the Kalman filter) to be consistent in the mean square sense is that there must be an increasing amount of information about the state **x** in the measurements. That is, as $k \to \infty$, the Fisher information must also tend to infinity. Figure 3 shows this for the monobot with constant parameters $P_{r,0|0}=Q=R=1$, and various sizes for the observation vector.

Notice how, as the total number of landmarks grows, the total Fisher information also grows, directly relating the number of landmarks to the amount of information available for state estimation in SLAM. Solving for the *k*-th sum term in **J** for the monobot,

$$J_k = \begin{bmatrix} \sum\sum \varsigma_{ij} & -\varsigma \\ -\varsigma^{\mathrm{T}} & S_k^{-1} \end{bmatrix} \tag{24}$$

with ς_{ij} the *ij*-th entry in S_k^{-1}, and $\varsigma = \left[\varsigma_{1i}, \dots, \sum \varsigma_{ni} \right]$
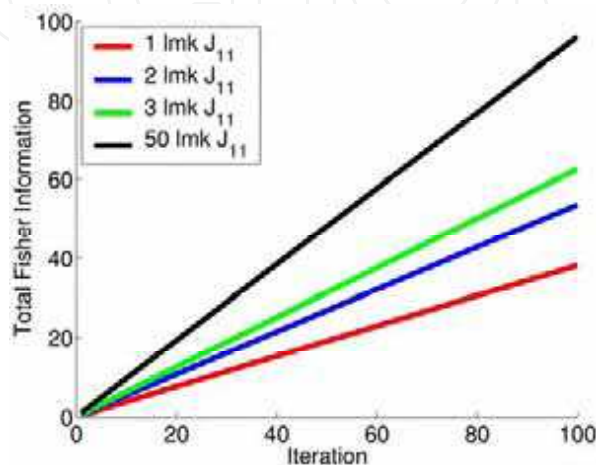

Figure 3. First entry in the total Fisher information matrix $\left(\sum\sum \varsigma_{ij} \right)$ for a monobot with variance parameters $P_{r,0|0}=Q=R=1$, and various sizes for the measurement vector

Citing Bar-Shalom (Bar-Shalom et al., 2001): "*a singular Fisher information matrix means total uncertainty in a subspace of the state space, that is, the information is insufficient for the estimation problem at hand*." Unfortunately, it can be easily shown, at least for the monobot case, that the first row (or column) of **J** is equivalent to the sum of the rest of the rows (or columns), producing a singular total Fisher information matrix. Thus, SLAM is unobservable.

This is a consequence of the form of the Jacobian **H**, i.e, of the full correlation in SLAM. Zero eigenvalues of $\mathbf{H}^{\mathrm{T}}\mathbf{S}^{-1}\mathbf{H}$ are an indicator of partial observability, and the corresponding vectors give the unobservable directions in state space.

So for example, for a one-landmark monobot, the innovation variance is the scalar (16), and since **H**=[-1,1], the Fisher information matrix in (23) evaluates to

$$J = \begin{bmatrix} 1 & -1 \\ -1 & 1 \end{bmatrix} \sum_{i=1}^{k} \frac{1}{s_i} \tag{25}$$

The unobservable direction of the state space is the eigenvector associated to the null eigenvalue of **J**, we denote it $\mathbf{E}_{\mathrm{Ker}\mathcal{O}}$ since it represents a basis for null space of the observability matrix $\mathcal{O}$, and evaluates to

$$\mathbf{E}_{\mathrm{Ker}\mathcal{O}} = \begin{pmatrix} 1 \\ 1 \end{pmatrix} \tag{26}$$

5. Relationship Between Observable and Controllable Subspaces for a Velocity Controlled Non-linear Planar Robot

We have developed closed form expressions for the bases of the observable and controllable subspaces in SLAM for a monobot and for a simple position controlled planar vehicle (Andrade-Cetto and Sanfeliu,).

In this Section we derive the observable and controllable subspace bases for the planar robot shown in Figure 4, a nonlinear nonholonomic velocity controlled wheeled vehicle with three degrees of freedom, and an environment consisting of two-dimensional point landmarks located on the floor.
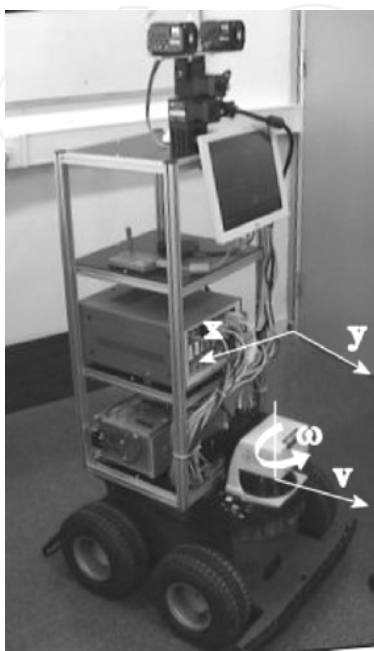

Figure 4. Two-dimensional mobile robot

The vehicle is controlled by a linear velocity v and a steering velocity ω. The process model used to predict the trajectory of the center of projection of the laser range scanner is given by

$$\begin{bmatrix} x_{k+1} \\ y_{k+1} \\ \theta_{k+1} \end{bmatrix} = \begin{bmatrix} x_k + \tau \left(\left(v_k + v_{v,k} \right) \cos \theta_k - \left(\omega_k + v_{\omega,k} \right) l \sin \theta \right) \\ y_k + \tau \left(\left(v_k + v_{v,k} \right) \sin \theta_k + \left(\omega_k + v_{\omega,k} \right) l \cos \theta \right) \\ \theta_k + \tau (\omega + v_{\omega,k}) \end{bmatrix} \quad (27)$$

where l is the distance from the center of the wheel axle to the center of projection of the laser range scanner, τ is the time constant, and v_v, v_ω are zero mean Gaussian model noises.

The observation model is

$$\begin{bmatrix} z_{r,k}^i \\ z_{\beta,k}^i \end{bmatrix} = \begin{bmatrix} \sqrt{\left(x_f^i - x_k \right)^2 + \left(y_f^i - y_k \right)^2} + w_{r,k} \\ \tan^{-1} \left(\dfrac{\left(y_f^i - y_k \right)}{\left(x_f^i - x_k \right)} \right) - \theta_k + \dfrac{\pi}{2} + w_{\beta,k} \end{bmatrix} \quad (28)$$

with z_r^i and σ the distance and bearing of an observed point landmark with respect to the laser center of projection. x_f^i and y_f^i are the absolute coordinates of such landmark, and i is used for the labelling of landmarks. $i=0$ indicates an anchor feature not under estimation in order to guarantee full observability. w_r and w_β are zero mean Gaussian measurement noises.

The Jacobian matrices **F**, **G**, and **H** are obtained by differentiating Equations (27) and (28) with respect to states and noises. That is,

$$F = \begin{bmatrix} 1 & 0 & -\tau((v_k + v_{v,k}) \sin \theta_k - l \cos \theta (\omega_k + v_{\omega,k})) & & 0 & 0 \\ 0 & 1 & \tau((v_k + v_{v,k}) \cos \theta_k - l \sin \theta (\omega_k + v_{\omega,k})) & & 0 & 0 \\ 0 & 0 & 1 & \ddots & 0 & 0 \\ 0 & 0 & 0 & & 1 & 0 \\ 0 & 0 & 0 & & 0 & 1 & \ddots \end{bmatrix} \quad (29)$$

$$G = \begin{bmatrix} \tau \cos \theta_k & -\tau l \sin \theta_k \\ \tau \sin \theta_k & \tau l \cos \theta_k \\ 0 & 1 \\ \vdots & \\ 0 & 0 \\ 0 & 0 \\ \vdots & \end{bmatrix} \quad (30)$$

$$H_i = \begin{bmatrix} -\dfrac{x_f^{(i)} - x_k}{d} & -\dfrac{y_f^{(i)} - y_k}{d} & 0 & \cdots & \dfrac{x_f^{(i)} - x_k}{d} & \dfrac{y_f^{(i)} - y_k}{d} & \cdots \\ \dfrac{y_f^{(i)} - y_k}{d^2} & -\dfrac{x_f^{(i)} - x_k}{d^2} & -1 & & \dfrac{y_f^{(i)} - y_k}{d^2} & \dfrac{x_f^{(i)} - x_k}{d^2} & \end{bmatrix} \quad (31)$$

with $d = \sqrt{\left(x_f^{(i)} - x_k \right)^2 + \left(y_f^{(i)} - y_k \right)^2} \; d = \sqrt{\left(x_f^{(i)} - x_k \right)^2 + \left(y_f^{(i)} - y_k \right)^2}$.

The dimensionality of the controllable subspace is dim x_r=3, and for the specific case in which only one landmark is available, a basis for the controllable subspace is simply

$$\mathbf{E}_{\mathrm{Im}\mathcal{C}} = \begin{pmatrix} \mathbf{I} \\ \mathbf{0}_{2\times 3} \end{pmatrix}$$

The dimensionality of the observable subspace is, for this particular configuration, rank $\mathcal{O}$=3. This last result is easily verified with simple symbolic manipulation of the expression resulting from substituting expressions (29) and (31) in the observability matrix

$$\mathcal{O} = \begin{bmatrix} \mathbf{H} \\ \mathbf{HF} \\ \vdots \\ \mathbf{HF}^{dim\mathbf{x}-1} \end{bmatrix} \tag{32}$$

Possible bases for $\mathrm{Im}\mathcal{O}^{\top}$, and for the null space of $\mathcal{O}$ (the unobservable subspace) are

$$\mathbf{E}_{\mathrm{Im}\mathcal{O}^{\top}} = \begin{pmatrix} 1 & 0 & 0 \\ 0 & 1 & 0 \\ 0 & 0 & 1 \\ -1 & 0 & 0 \\ 0 & -1 & 0 \end{pmatrix} \quad \mathbf{E}_{\mathrm{Ker}\mathcal{O}} = \begin{pmatrix} 1 & 0 \\ 0 & 1 \\ 0 & 0 \\ 1 & 0 \\ 0 & 1 \end{pmatrix}$$

The only independently observable state is the one associated to the robot orientation ϕ. The other four states, the Cartesian coordinates of the robot and landmark locations span a space of dimension 2. Even when $\mathrm{Im}\mathcal{C}$ and $\mathrm{Im}\mathcal{O}^{\top}$ both span $\mathbb{R}^3$, we see that the inequality $\mathrm{Im}\mathcal{C} \neq \mathrm{Im}\mathcal{O}^{\top}$ still holds, as in the case of the monobot. That is, the observable and controllable subspaces for this one-landmark 3dof-robot SLAM problem correspond to different three-dimensional subspaces in $\mathbb{R}^5$; and, their intersection represents the only fully controllable and observable state, i.e., the robot orientation.

6. Complete Observability

In Section 4 we characterized the unobservable subspace in SLAM as the subspace spanned by the null eigenvectors of the total Fisher information matrix. Furthermore, we showed in Section 5 how the unobservable part of the state space is precisely a linear combination of the landmark and robot pose estimates.

In order to gain full observability we propose to extend the measurement model doing away with the constraint imposed by full correlation by letting one landmark serve as a fixed global reference, with its localization uncertainty independent of the vehicle pose. The principle behind is that full observability requires an uncorrelated measurement Jacobian, or equivalently, a full rank Fisher information matrix. The use of a fixed global reference as anchor guarantees that.

The measurement model of a global reference fixed at the origin, for the nonlinear vehicle from Figure 4. is

$$h^{(0)} = \begin{bmatrix} \sqrt{x_k^2 + y_k^2} + w_{r,k} \\ \tan^{-1}\left(\dfrac{y_k}{x_k}\right) - \theta_k + \dfrac{\pi}{2} + w_{\beta,k} \end{bmatrix} \tag{33}$$

and its corresponding Jacobian is

$$H_0 = \begin{bmatrix} \dfrac{x_k}{\sqrt{x_k^2 + y_k^2}} & \dfrac{y_k}{\sqrt{x_k^2 + y_k^2}} & 0 & 0 & 0 & \cdots \\[3mm] -\dfrac{y_k}{x_k^2 + y_k^2} & \dfrac{x_k}{x_k^2 + y_k^2} & -1 & 0 & 0 & \end{bmatrix} \tag{34}$$

The symbolic manipulation of

$$H = \begin{bmatrix} H_0 \\ H_i \end{bmatrix} \tag{35}$$

with a commercial algebra package, produces a full rank observability matrix. That is, for the linearized nonholonomic velocity controlled planar mobile robot platform used, the simultaneous measurement of one anchor as global reference, and any other landmark, is sufficient to attain full observability in SLAM.

7. Suboptimal Filter Stability

When a stochastic system is partially controllable, such as in the case of SLAM, the Gaussian noise sources v_k do not affect all of the elements of the state space. The diagonal elements of **P** corresponding to these incorruptible states will be driven to zero by the Kalman filter, and once this happens, these estimates will remain fixed and no further observations will alter their values. The dynamics of the model assume the landmarks are fixed elements, for which no process noise is considered. Therefore, their associated noise covariance (its determinant) will asymptotically tend to zero (Dissanayake et al., 2001). The filter gain for the landmark states will also tend to zero. Figure 5 shows two new simulations for a linear SLAM case, a monobot under Brownian motion with one and two landmarks. The simulations show the evolution of the localization errors for both the monobot and the landmarks, and the reduction of the landmark part of the Kalman gain, due to the uncontrollability of the system. The only way to remedy this situation is to add a positive definite pseudo-noise covariance to those incorruptible states (Bar-Shalom et al., 2001).

In Figure 5, the vehicle location is indicated by the darkest curve at the -1m level in the first row of plots. In the same set of plots, and close to it, is a lighter curve indicating the vehicle location estimate as computed by the filter, along with 2σ bounds on such estimate shown as dotted lines. The dark straight lines at the 1m level indicate the landmark location estimates; and the lighter curves are noise corrupted signals of sensor measurements. Also shown, are a pair of dotted lines for 2σ bounds on the landmark location estimates. The second row of plots shows the vehicle location error only, and its corresponding variance, also on the form of 2σ dotted bounds.

See how the localization error has non-zero mean due to partial observability, an undesirable feature in Kalman filtering. The third row shows non-zero mean landmark state estimate errors. And, the last row shows the Kalman filter gains both for the vehicle and landmark revision terms. The Kalman gains for the revision of the landmark estimates rapidly tend to zero, the reason being that these states are uncontrollable.
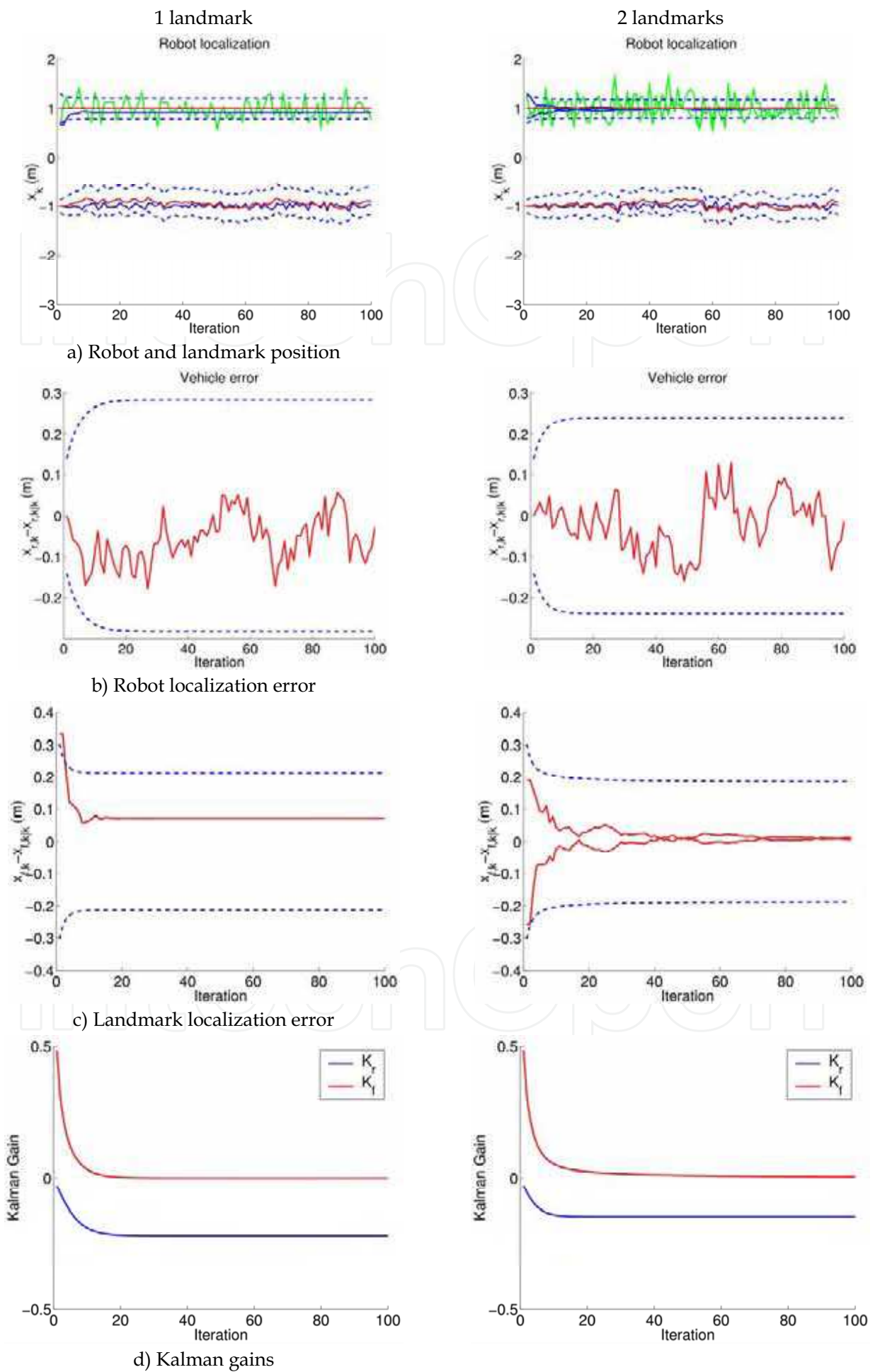
1 landmark

2 landmarks

a) Robot and landmark position

b) Robot localization error

c) Landmark localization error

d) Kalman gains

Figure 5. Partially observable SLAM for a monobot during Brownian motion with 100 iterations (see text)

7.1 *O*(*N*) but Unstable Partially Observable SLAM

One way to add pseudo-noise to the model is by diagonalizing the state error covariance matrix (Guivant and Nieto, 2001, 2003, Julier, 2003). This technique is often used to reduce the time complexity of the algorithm from O(N^2) to *O*(*N*). The result is a suboptimal filter that will compute inflated estimates for the vehicle and landmark covariances, that has the computational advantage of being uncorrelated. The addition of a covariance term $\Delta \mathbf{P}$ to the a priori state covariance estimate

$$P_{k+1|k} = FP_{k|k}F^{\mathrm{T}} + GQG^{\mathrm{T}} + \Delta P \tag{36}$$

is equivalent to providing a new form to the plant noise Jacobian $G' = \begin{bmatrix} G & I \end{bmatrix}$

$$P_{k+1|k} = FP_{k|k}F^{\mathrm{T}} + G'\begin{bmatrix} Q & \\ & \Delta P \end{bmatrix}G'^{\mathrm{T}} \tag{37}$$

$\Delta \mathrm{P}$ may be chosen, for example, such as to minimize the trace of a resulting block diagonal P in (36) (Julier, 2003).

Choosing a full rank $\Delta \mathrm{P}$ is equivalent to having noise input to more states than those that can be observed with the filter. In this case, because of partial observability, both vehicle and landmark variance estimates become unbounded. Figure 6 shows this for the same monobot experiment as in the previous simulation. This phenomena was first observed in (Julier, 2003) using relative maps. Not only both the vehicle and landmark state estimation variances become unbounded. Also, thanks to the full controllability of the system, the Kalman gain for the revision of the landmark states is greater than zero; but still, does not converge to a steady state value. We believe that the addition of pseudo-noise should be performed only at most, in the amount of states equal to the dimension of the observable subspace.

7.2 O(N) and Stable Partially Observable SLAM

One solution to the problem of instability during covariance inflation, is to decorrelate only the landmark state estimates, and to preserve all vehicle to landmark correlations (Vidal-Calleja et al., 2004a).

$$\Delta P = \begin{bmatrix} 0 & \\ & Q_f \end{bmatrix} \tag{38}$$

such that P$_f$ +Q$_f$, the map part of the state error covariance, is block diagonal.

Figure 7 shows a partially observable monobot under Brownian motion for which only the landmark part of the state error covariance matrix has been decorrelated. The algorithm does converge to a steady state solution under this circumstances, and still can be implemented in real time. The one landmark case is identical than the original case, since a linear one landmark map is already diagonal (scalar actually).

For the two-landmark case, the landmark variance estimate is greater than the optimal solution shown in the third column in Figure 5 since the covariance has been inflated during decorrelation. Furthermore, now that the system is controllable, the Kalman gains for the landmark state estimates do not become zero, and they converge to a steady state value.

Moreover, we $\mathcal{O}$, that the covariance inflation suboptimal partially observable SLAM converges only when

$$\mathrm{rank}\ \varDelta \mathrm{P}\ \le \mathrm{rank}\ \mathcal{O} \tag{39}$$

1 landmark

2 landmarks

a) Robot and landmark position

b) Robot localization error
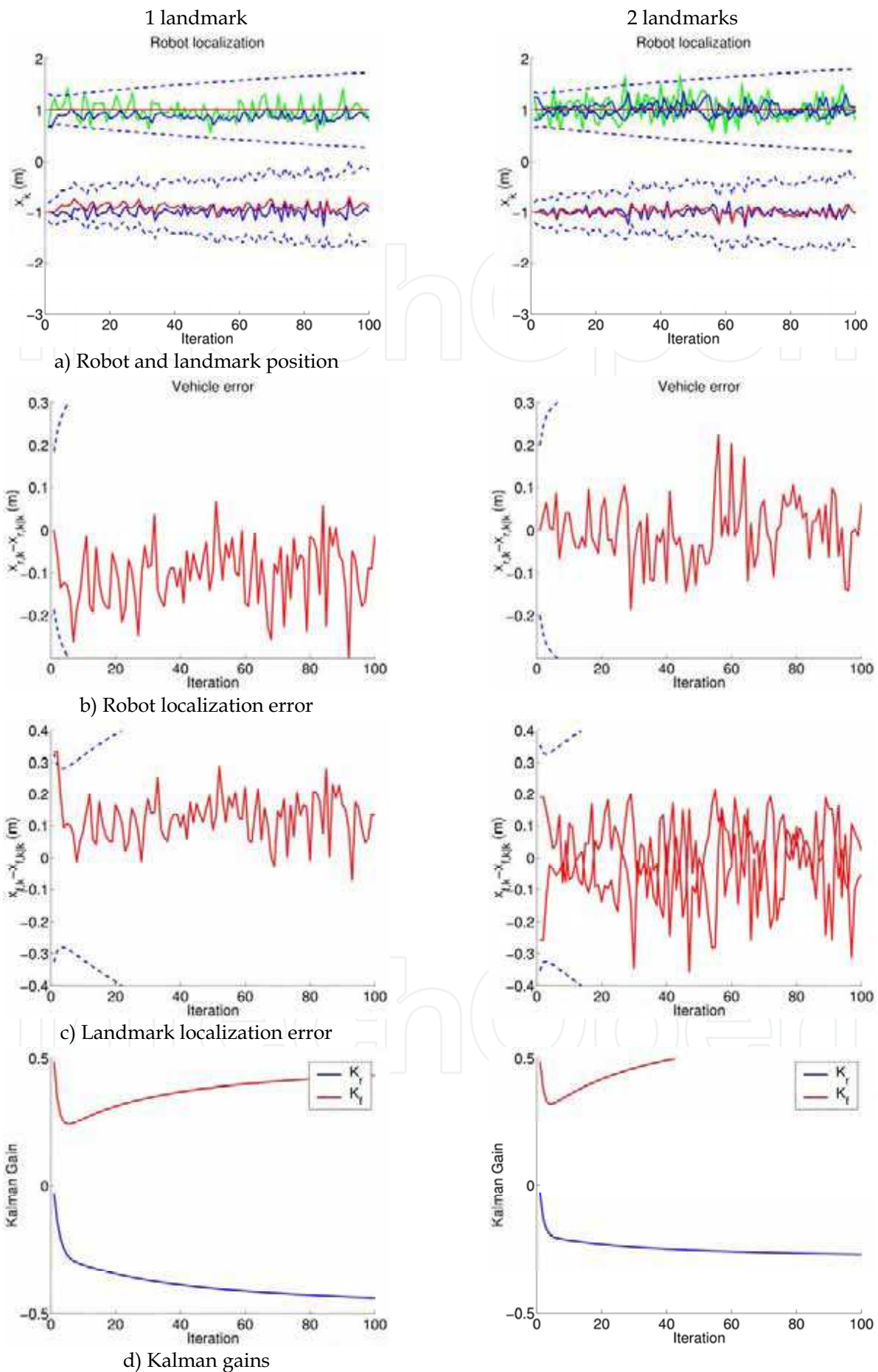

c) Landmark localization error

d) Kalman gains

Figure 6. Partially observable SLAM for a Brownian motion monobot with 100 iterations. The entire state error covariance is decorrelated with the minimal trace solution (Julier, 2003). By decorrelating the entire state error covariance matrix, the covariance estimates become unbounded
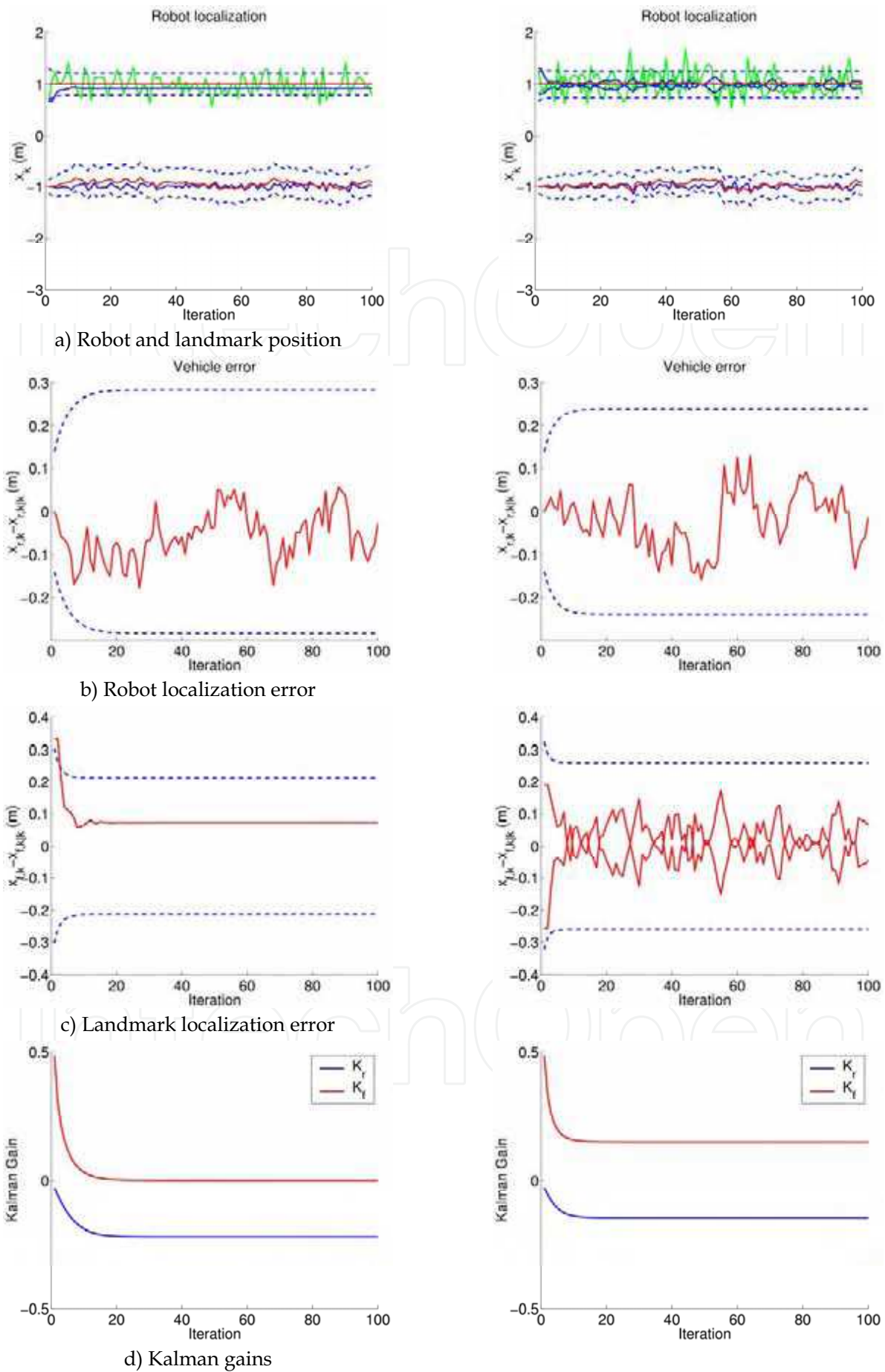
a) Robot and landmark position

b) Robot localization error

c) Landmark localization error

d) Kalman gains

Figure 7. Partially observable SLAM for a Brownian motion monobot with 100 iterations. The state error covarance is decorrelated only for the landmark part of the state vector, with the minimal trace solution. By decorrelating only the map part of the state error covariance matrix, we preserve filter stability

b) Vehicle error

c) Landmark localization error

d) Kalman gains
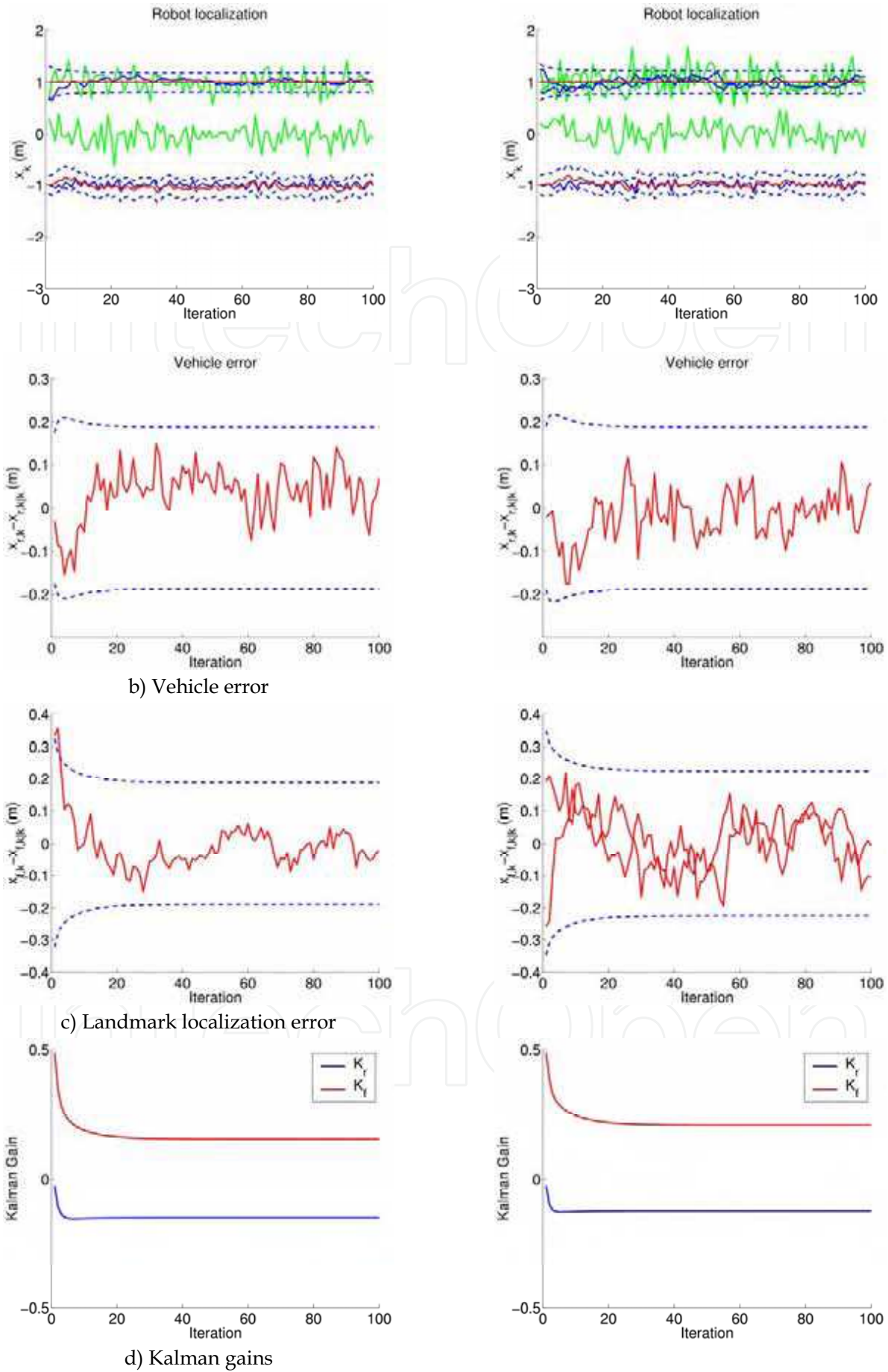
Figure 8. Fully observable SLAM for a Brownian motion monobot with 100 iterations. The entire state error covarance is decorrelated with the minimal trace solution. In the linear case, it is possible to decorrelate the entire state error covariance matrix, and still preserve filter stability

a) Vehicle localization error   b) Vehicle covariance

c) Landmark localization errors   d) Landmark covariance
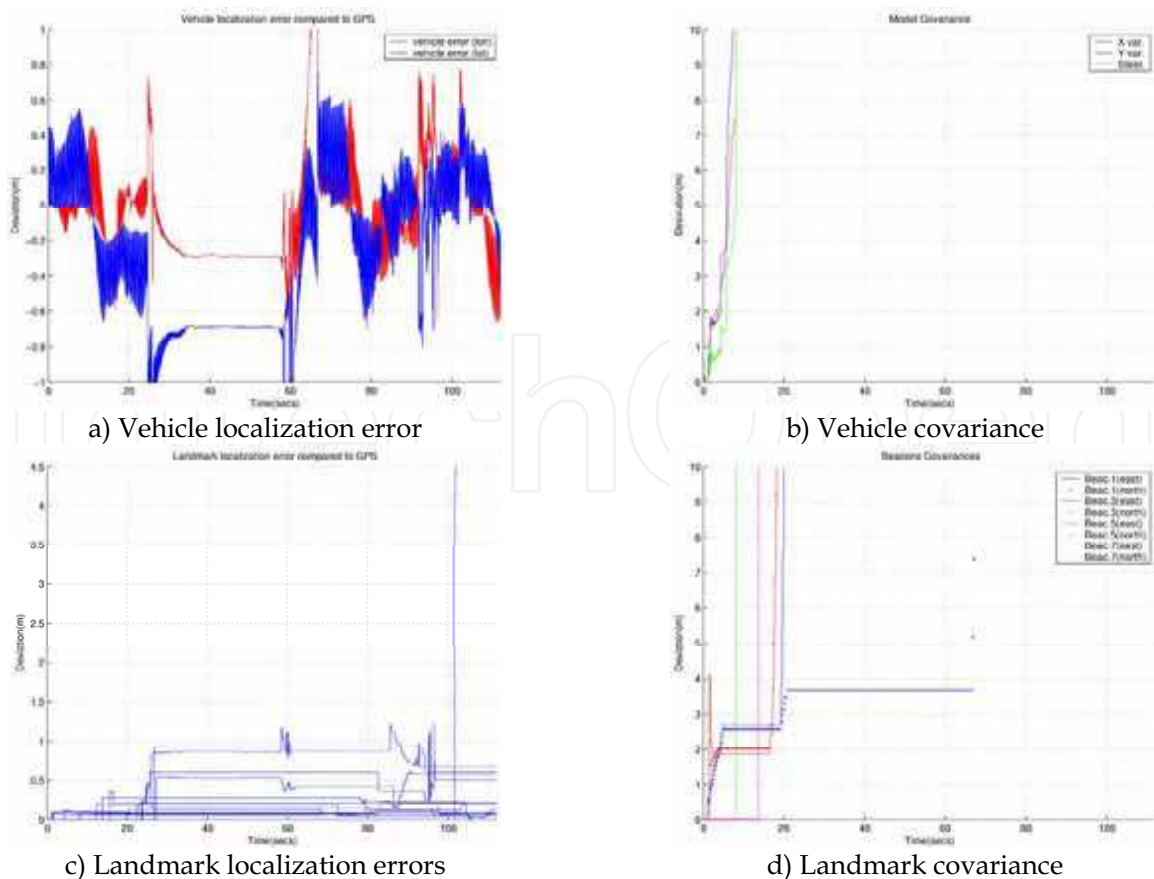
Figure 9. Partially observable SLAM for a car-like vehicle at the University of Sydney Car Park. The entire state error covariance matrix is decorrelated with the minimal trace solution (Julier, 2003)

7.3 O(N) and Stable Fully Observable SLAM

Consider now the fully observable case from the previous Section. If we add pseudo-noise to the vehicle as well as to the landmark states, the covariance will reach a steady-state value, and the Kalman gain will not be zero, at least, in the linear case. Figure 8 shows this results diagonalizing the whole state error covariance (not only the landmark part of $\mathbf{P}$).
In this latter experiment, the state error variances reach lower values than those in the partially observable case. The solution of the Riccati equation is now independent of the initial covariance estimate $\mathbf{P}_{0|0}$. We have observed experimentally however, that with a nonlinear vehicle model, it is best to also decorrelate only the map part of the state error covariance, even in the fully observable case.

7.4 Experimental Results

We show now results on a series of experiments for a nonlinear vehicle with an also nonlinear measurement model, using the ACFR - University of Sydney database (Nebot et al., 2002). The test run used corresponds to a car-like vehicle at the University Car Park. The landmarks used are tree trunks, as measured with a laser range finder. The reconstructed maps are compared to GPS ground truth for accuracy. The first experiment corresponds to a typical partially observable SLAM run, in which the entire state error covariance is being decorrelated as discussed in Section 7.1. Figure 9 plots results on this run, showing in rows b) and d) unbounded covariances both for the vehicle and landmark state estimates, due to the naïve covariance inflation method used.

The second experiment corresponds to the same partially observable SLAM conditions, but decorrelating only the map part of the state error covariance. Adding pseudo-noise to the landmark states during the inflation procedure amounts to making the system controllable; and doing so for as many states as those observable, produces both vehicle and landmark bounded state covariance estimates. This is shown in Figure 10, frames b) and d). Figure 12 frame a) shows the actual vehicle path and landmark location estimates recovered by the algorithm, compared to GPS ground truth for the beacons. Note that even when the "relative" map is consistent (Dissanayake et al., 2001), it is slightly rotated and shifted from the actual beacon locations. The amount of this shift depends on the initial vehicle uncertainty, i.e., the initial filter conditions, and can be seen in Figure 10, frame c).

The last experiment shown corresponds to a fully observable SLAM run (using the first observed beacon as an anchor), and also decorrelating only the map part of the state error covariance. In this case, the vehicle and landmark covariance estimates do not depend on the initial filter conditions, and thus are significantly reduced. This is shown in frames b) and d) in Figure 11. The absolute landmark estimate error is also significantly reduced, as shown in Figure 11, frame c). Figure 12 frame b) shows the actual vehicle path and landmark estimates as recovered by the filter. The beacon shown in the center of the plot is used as an anchor to the map, and no state estimate is computed for it. This last map was obtained with a suboptimal linear-time SLAM algorithm that has both bounded covariance estimates, and independence on the filter initial conditions; thus producing a fast and accurate absolute map.

a) Vehicle localization error   b) Vehicle covariance

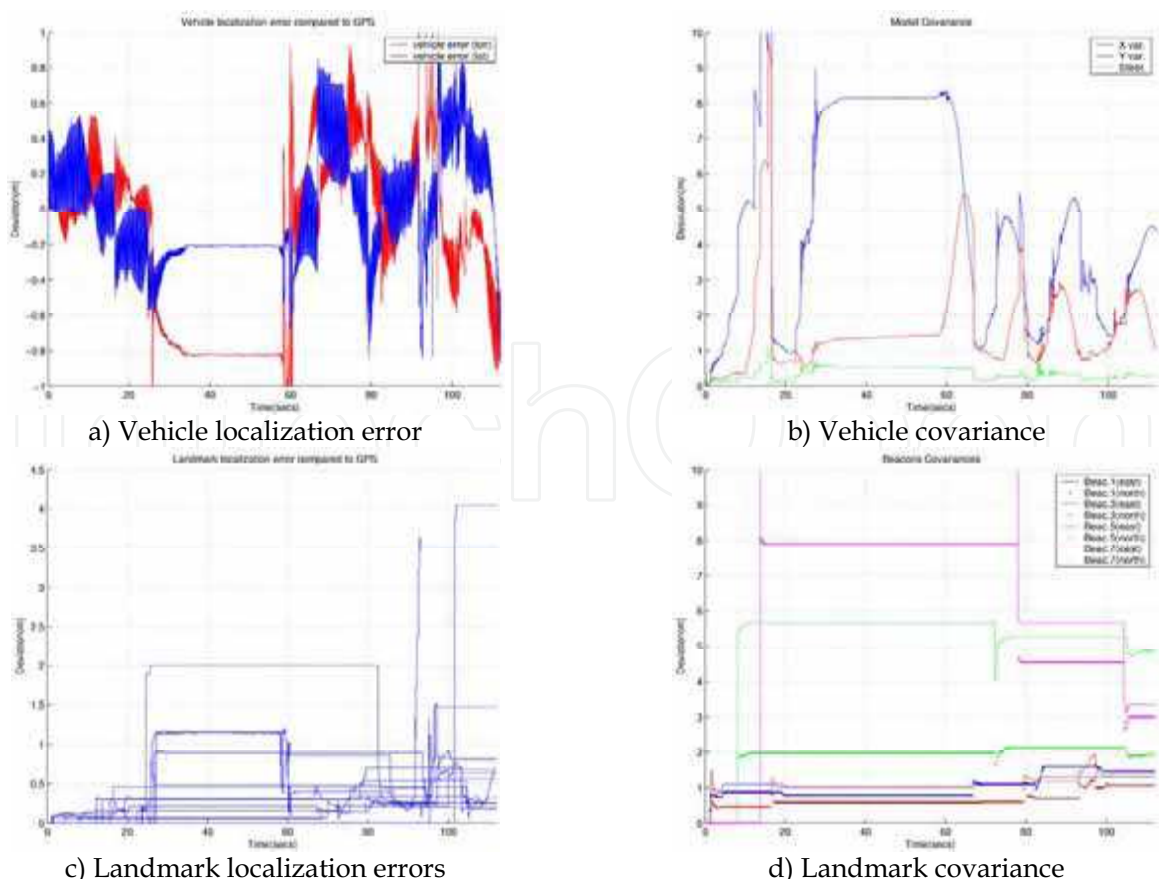c) Landmark localization errors   d) Landmark covariance

Figure 10. Partially observable SLAM for a car-like vehicle at the University of Sydney Car Park. Only the map part of the state error covariance matrix is decorrelated with the minimal trace solution. By adding controllability to as many states as those that are observable, the filter remains stable, and the estimated covariances remain bounded

a) Vehicle localization error

b) Vehicle covariance

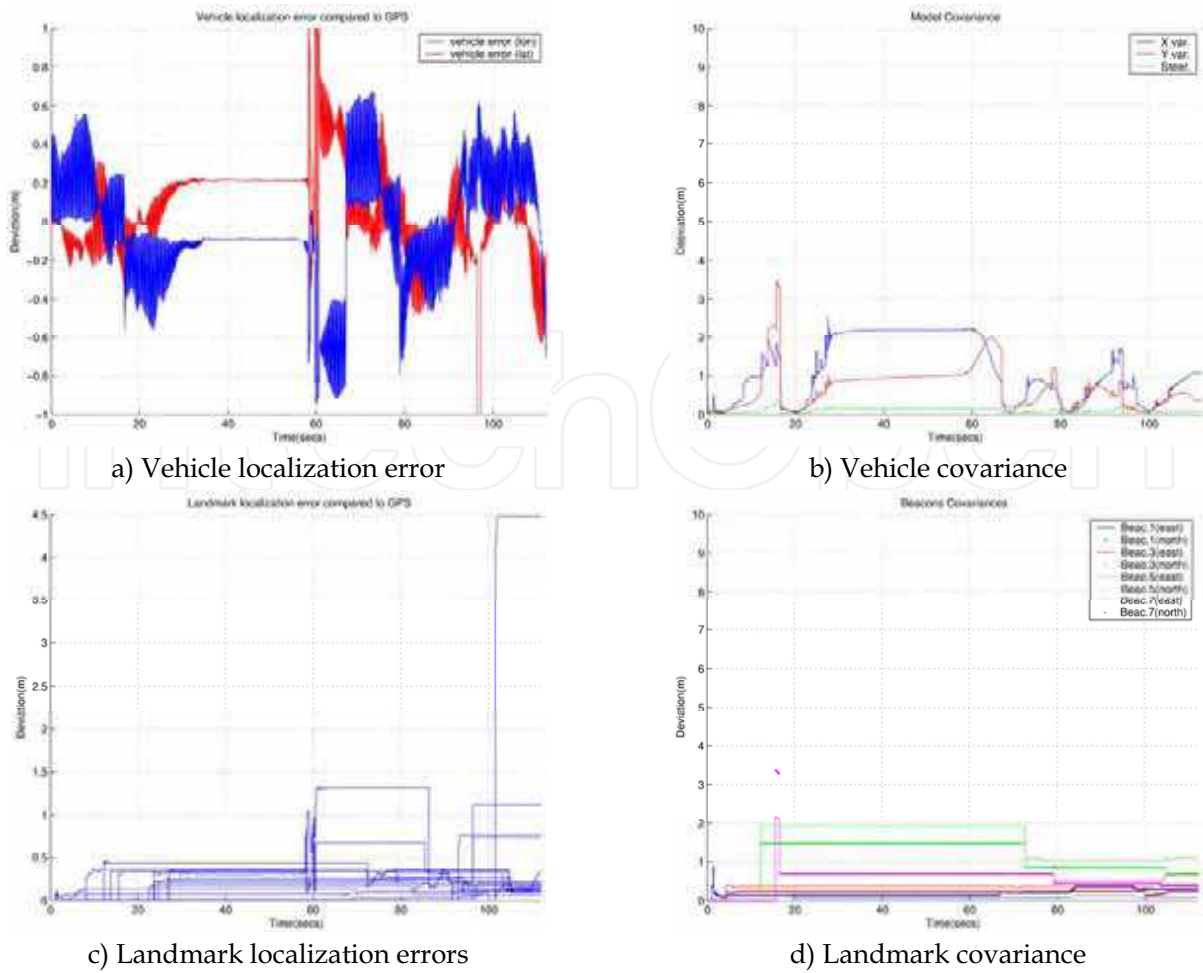c) Landmark localization errors

d) Landmark covariance

Figure 11. Fully observable SLAM for a car-like vehicle at the University of Sydney Car Park. Only the map part of the state error covariance is decorrelated with the minimal trace solution. Full observability guarantees independence of the filter initial conditions, and an accurate absolute map is obtained, with smaller covariance estimates than its relative counterpart
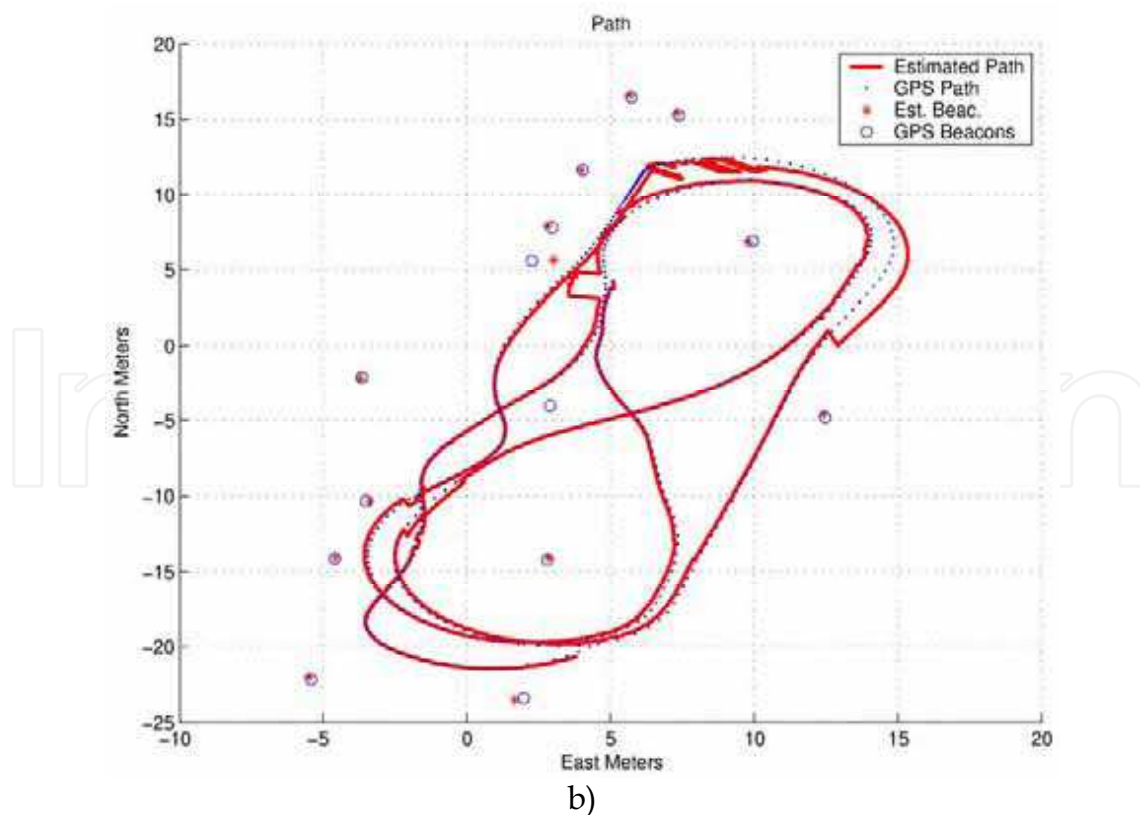

a)

b)
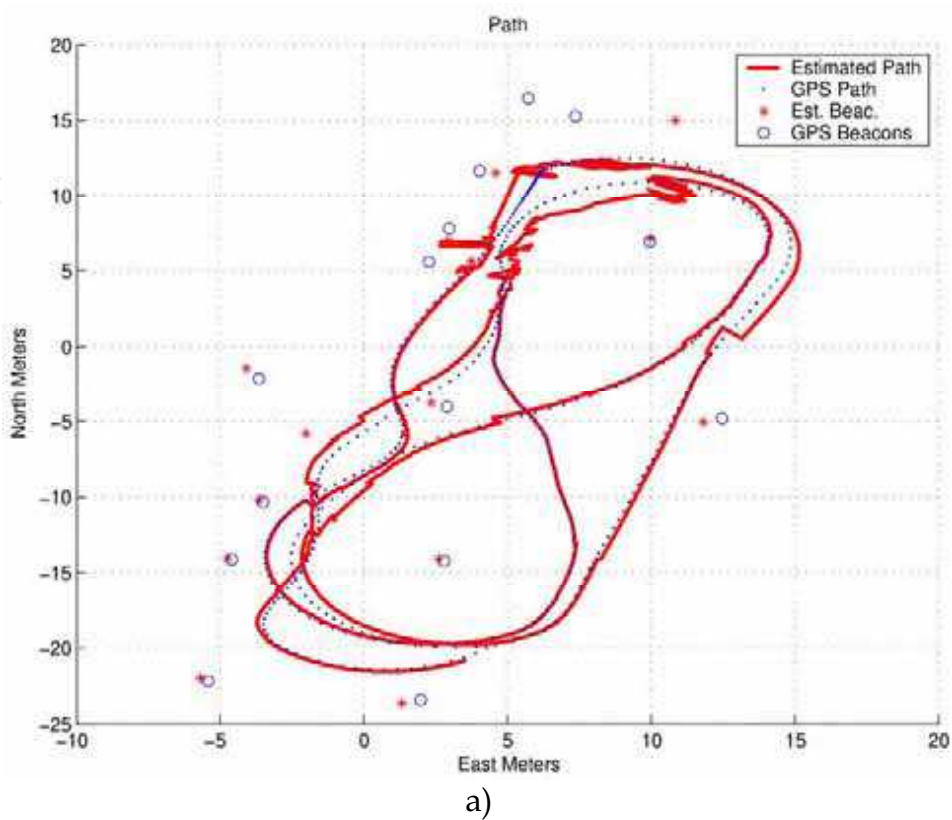
Figure 12. Vehicle path and landmark location estimates, compared to GPS ground truth for an a) partially observable suboptimal SLAM run, and a b) fully observable suboptimal SLAM run; both with decorrelation of only the map part of the state error covariance matrix

8. Conclusions

We have shown that full correlation of the map model in the Kalman Filter based approach to Simultaneous Localization and Map Building hinders full observability of the state estimate. A unit norm eigenvalue for the matrix **F-KH** makes the state error estimate converge to a non zero mean constant bounded value in the linear case SLAM. Marginal stability of such partially observable system produces also at least one *psd* solution to the steady state Riccati equation for the covariance error, provided the initial conditions of **P** are also *psd*. Partial observability makes the final map dependant on the initial observations. This situation can easily be remedied either by anchoring the map to the first landmark observed, or by having an external sensor that sees the vehicle at all times.

Suboptimal techniques to improve the speed of the algorithm include covariance inflation methods to diagonalize the state error covariance matrix. These techniques may lead to instability if pseudo-noise is added in a higher state dimensionality than what can be observed. We propose in this Chapter to diagonalize only the map part of the state error covariance, thus guaranteeing convergence of **P**, and at the same time obtaining an $O(N)$ algorithm.

9. References

J. Andrade-Cetto and A. Sanfeliu. The effects of partial observability when building fully correlated maps. To appear in *IEEE Transactions on Robotics*.

Y. Bar-Shalom, X. Rong Li, and T. Kirubarajan. *Estimation with Applications to Tracking and Navigation*. John Wiley & Sons, New York, 2001.

M. W. M. G. Dissanayake, P. Newman, S. Clark, H. F. Durrant-Whyte, and M. Csorba. A solution to the simultaneous localization and map building (SLAM) problem. *IEEE Transactions on Robotics and Automation*, 17 (3):229–241, June 2001.

P. W. Gibbens, G. M. W. M. Dissanayake, and H. F. Durrant-Whyte. A closed form solution to the single degree of freedom simultaneous localisation and map building (SLAM) problem. In *Proceedings of the IEEE International Conference on Decision and Control*, pages 408–415, Sydney, December 2000.

J. E. Guivant and E. M. Nieto. Optimization of simultaneous localization and map-builidng algorithm for real-time implementation. *IEEE Transactions on Robotics and Automation*, 17 (3):242–257, June 2001.

J. E. Guivant and E. M. Nieto. Solving computational and memory requirements of feature-based simultaneous localization and mapping algorithms. *IEEE Transactions on Robotics and Automation*, 19 (4):749–755, August 2003.

S. J. Julier. The stability of covariance inflation methods for SLAM. In *Proceedings of the IEEE/RSJ International Conference on Intelligent Robots and Systems*, pages 2749–2754, Las Vegas, October 2003.

T. Kailath, A. H. Sayed, and B. Hassibi. *Linear Estimation*. Information and System Sciences Series. Prentice Hall, Upper Saddle River, 2000.

S. J. Kim. *Efficient Simultaneous Localization and Mapping Algorithms using Submap Networks*. PhD thesis, Massachusetts Institute of Technology, Cambridge, June 2004.

E. Nebot, J. Guivant, and J. Nieto. ACFR, experimental outdoor dataset, 2002.

J. Neira and J. D. Tardós. Data association in stochastic mapping using the joint compatibility test. *IEEE Transactions on Robotics and Automation*, 17 (6):890–897, December 2001.

R. C. Smith and P. Cheeseman. On the representation and estimation of spatial uncertainty. *International Journal of Robotics Research*, 5 (4):56–68, 1986.

R. Todling. Estimation theory and foundations on atmosferic data assimilation. Technical Report DAO Note 1999-01, Data Assimilation Office. Goddard Space Flight Center, 1999.

T. Vidal-Calleja, J. Andrade-Cetto, and A. Sanfeliu. Conditions for suboptimal filter stability in SLAM. In *Proceedings of the IEEE/RSJ International Conference on Intelligent Robots and Systems*, volume 1, pages 27–32, Sendei, September 2004a.

T. Vidal-Calleja, J. Andrade-Cetto, and A. Sanfeliu. Estimator stability analysis in SLAM. In *Proceedings of the 5th IFAC/EURON Symposium on Intelligent Autonomous Vehicles*, Lisbon, July 2004b.

Cutting Edge Robotics

Edited by Vedran Kordic, Aleksandar Lazinica and Munir Merdan

This book is the result of inspirations and contributions from many researchers worldwide. It presents a collection of wide range research results of robotics scientific community. Various aspects of current research in robotics area are explored and discussed. The book begins with researches in robot modelling & design, in which different approaches in kinematical, dynamical and other design issues of mobile robots are discussed. Second chapter deals with various sensor systems, but the major part of the chapter is devoted to robotic vision systems. Chapter III is devoted to robot navigation and presents different navigation architectures. The chapter IV is devoted to research on adaptive and learning systems in mobile robots area. The chapter V speaks about different application areas of multi-robot systems. Other emerging field is discussed in chapter VI - the human- robot interaction. Chapter VII gives a great tutorial on legged robot systems and one research overview on design of a humanoid robot.The different examples of service robots are showed in chapter VIII. Chapter IX is oriented to industrial robots, i.e. robot manipulators. Different mechatronic systems oriented on robotics are explored in the last chapter of the book.

How to reference

In order to correctly reference this scholarly work, feel free to copy and paste the following:

INTECH
open science | open minds